Nanoscale

Accepted Manuscript

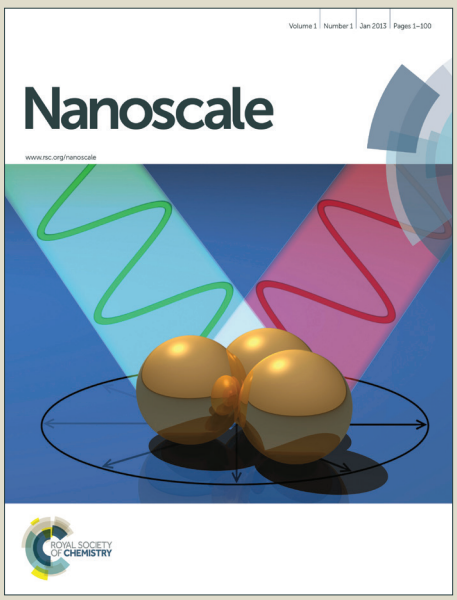

ROYAL SOCIETY OF CHEMISTRY

www.rsc.org/nanoscale

Large Pore Mesoporous Silica Nanomaterials for Application in Delivery of Biomolecules

Nikola Ž. Knežević,[a,b]* Jean-Olivier Durand[b]

a *Faculty of Pharmacy, European University, Trg mladenaca 5, 21000 Novi Sad, Serbia*

b Institut Charles Gerhardt Montpellier, UMR 5253 CNRS-UM2-ENSCM-UM1, CC1701 Equipe Chimie Moléculaire et Organisation du Solide, Place Eugène Bataillon, 34095 Montpellier Cedex 05, France

*Corresponding author; email:nikola.knezevic@faculty-pharmacy.com

Abstract

Various approaches for the synthesis of mesoporous silicate nanoparticles (MSN) with large pore (LP)-diameters (in the range of 3-50 nm) are reviewed in this article. The work also covers construction of magnetic analogues of large pore-mesoporous silica nanoparticles (LPMMSN) and their biomedical applications. The constructed materials exhibit vast potential for application in loading and delivery of large drug molecules and biomolecules. Literature reports on application of LPMSN and LPMMSN materials for adsorption and delivery of proteins, enzymes, antibodies and nucleic acids are covered in depth, which exemplify their highly potent characteristics for use in drug and biomolecule delivery to diseased tissues.

Introduction

The research field of mesoporous silica nanomaterials has been rapidly expanding during the past two decades, which consequently led to branching of the original research area into separate categories encompassing different structures of the materials. Based on the particle size, the silicate materials can be classified to macroscopic (monolithic) materials,[1] microparticulate

materials[2] and nanoparticulate materials.[3] While the materials belonging to the first two categories find extensive application in separation and catalysis, the nanoparticulate mesoporous silicates (MSN) are especially suitable for biomedical applications. The porous structure of the MSN materials may differ as well in dependence of the employed synthesis conditions and hence materials with hollow interiors,[4] or nanoparticles containing hexagonal,[3] cubic[5] and radial[6] arrangements of the mesopores may be observed. Vast majority of contemporary MSN materials are synthesized by cetyltrimethylammonium bromide (CTAB)-templated silica condensation in basic aqueous environment, which typically yield materials with pore diameters of up to 3 nm. However, it is possible to construct materials with pore sizes larger then this value, large-pore MSN (LPMSN), which exhibit supremacy over smaller pore-MSN with regards to mass transfer, diffusivity, and penetration ability of large drug molecules, proteins or nucleic acids into or out of the pore system. For example, it has been shown in an early report that expansion of the pore diameter of mesoporous silicates increases the rate of drug delivery.[7] The authors compared ibuprofen delivery from mesoporous silicates of different pore diameters and by decreasing the pore diameter from 3.6 to 2.5 nm the results revealed fivefold decrease in the rate of drug release. The result is attributed to slower diffusion rate of the solvent into the mesopores and slower counterdiffusion of the drug to the bulk solution in case of pores with smaller diameter. In addition, the obtained results revealed that materials with wider mesopores exhibited higher amounts of loaded and delivered drug per unit of specific surface area of the material due to better packing efficiency of the drug inside the wider mesopores. Hence, research on LPMSN materials is of substantial interest for increasing the loading and delivery capacity of drug/biomolecule carriers as well.

There are generally two pathways for the synthesis of large pore-mesoporous silicate materials. One is to expand the surfactant templated pores with suitable organic molecules, serving as auxiliary templating agent, while the second pathway is to utilize amphiphilic copolymers or surfactants with longer hydrophobic chains, to serve for pore-templating, Biocompatibility of MSN-type materials, their biodistribution and applicability for *in vivo* targeted treatment of cancer has been previously demonstrated.[8,9] Large pore-analogs of MSN have been recently applied as well to monitor the biodistribution of the nanoparticles *in vivo* by positron emission tomography (PET).[10] Expanded mesopores were needed for construction of this imaging nanomaterial in order to increase the amount of the covalently attached large ligand for the positron emitting zirconium-89, inside the mesopores. The large pores of the material were obtained by postsynthetic hydrothermal treatment with trioctylphosphine oxide (TOPO) at 398 K for 3 days. Evidently, after this process the average pore diameter changed from the initial 3.5 nm to 8 nm but the surface area expectedly decreased from 1236 m^2/g to 407 m^2/g.

One of the most attractive areas for biomedical application of LPMSNs is in construction of growth factor-loaded systems for tissue regeneration. Of particular importance is regeneration of neural tissues, in order to restore normal functions of diseased or injured central and peripheral nervous system. A progress in this research area has been made by developing conductive polypyrrol (Ppy) polymer matrix which contains embedded LPMSN with mesopore-loaded nerve growth factor (NGF).[11] The large pores of the material (4.71 nm) were obtained by addition of mesitylene (1,3,5-trimethylbenzene = TMB) as the pore-expanding agent to the CTAB-templated synthesis of MSN material, in the presence of ammonia. The authors studied growth and development of PC 12 cells on the surface of Ppy matrix, Ppy matrix containing empty LPMSN and Ppy matrix containing NGF-loaded LPMSN. The results revealed that presence of

NGF/LPMSN significantly improved the proliferation of the cells due to steady release of NGF. Moreover, the presence of NGF stimulated development of neurite extensions, which were even more pronounced by electrical stimulation, which caused contraction and expansion of the Ppy matrix and hence promotion of NGF release. NGF-containing LPMSNs were also recently embedded in a collagen gel and the system was also proven to promote proliferation and formation of neurite extensions on PC 12 cells.[12] Furthermore in this study the cells were grown in the 3D collagen matrix, which is a step further toward tissue engineering and application in neural regeneration. LPMSN material, applied in this study, was synthesized by application of triocetylmethylammonium bromide (TOMAB) as an auxiliary pore – templating surfactant, along with CTAB, with the presence of ammonia in ethanol/water mixture. Size of the nanoparticles was around 300 nm in diameter with high surface area (1265 m^2/g) and with bimodal pore size distribution (15.9 and 2.31 nm). The authors also demonstrated in this study that small pore-MSN with similar characteristics exhibited much lower capacity for loading proteins. Hence, in light of the attractive examples of usefulness of LPMSN materials we overview various strategies employed for the construction of LPMSNs and their biomedical applications.

Early Efforts in Synthesis and Application of Large Pore Mesoporous Silicates

Since the first reports on mesoporous silica materials (MCM-41 = Mobil Composition of Matter No. 41) by Kresge et al. at Mobil company,[2,13] the possibility to obtain materials with different pore diameters was demonstrated by changing the surfactant template or by addition of auxilliary templating molecules. In these early reports the authors obtained materials with hexagonally packed mesopores of less than 4 nm in diameter by using CTAB as the mesopore-template in

basic environment. However, the authors also demonstrated application of mesitylene as the pore-swelling agent and the synthesized materials showed pored diameters of up to 10 nm.

Another silica material with hexagonal packing of the mesopores (SBA-15 = Santa Barbara Amorphous No. 15), which was developed by Zhao, Stucky et al. by using amphiphilic block copolymers as organic structure-directing agents,[14] can be as well synthesized with different pore diameters.[15] Herein the addition of TMB to the mesopore-templating block copolymer consisting of: poly(ethylene oxide)– poly(propylene oxide)–poly(ethylene oxide) (PEO-PPO-PEO) before silica condensation in acidic environment, was shown to produce SBA-15 materials with mesopores as wide as 30 nm in hexagonally structured microparticles. For example, SBA-15 prepared with a TMB : $PEO_{20}PPO_{70}PEO_{20}$ (i.e. Pluronic P-123) weight ratio of 3:4 is a thermally stable material with BET surface area of 910 m^2/g and hexagonally packed mesopores with an average pore size of 26 nm and pore volume of 2.2 cm^3/g. Without addition of TMB various templating PEO-PPO-PEO or PPO-PEO-PPO block copolymers in different conditions produced materials with average pore diameters up to 10 nm. Interestingly, if TMB and Pluronic P-123 were used as co-templates in a different synthetic procedure the obtained material was mesocellular siliceous foam (MCF), which contained pore diameters in the range 17 – 42 nm.[16] Finally the authors reported application of SBA-15 and MCF materials for adsorption and release of proteins.[17] Adsorption of negatively charged proteins of different sizes was achieved on positively charged amine-functionalized surface of large pore-MCF (16 nm) and smaller pore-SBA-15 (5.9 nm). SDS PAGE electrophoresis of the supernatants, after inducing the release of proteins from the materials by increasing ionic strength, revealed that the materials exhibited size exclusion behavior. While MCF material was capable of adsorbing and releasing all of the tested proteins, SBA-15 was capable of adsorbing and releasing only the protein with the smallest size.

However, application of large pore-SBA-15 material in HPLC separation of biomolecules was successfully demonstrated.[18]

Takahashi et al. reported comparison of TMB or 1,3,5-triisopropybenzene-swelled FSM-16 (folded sheet mesoporous) material and MCM-41 (both synthesized by surfactant template method in basic solution) vs. SBA-15 material in terms of the surface adsorption capability of horseradish peroxidase (HRP) and subtilisin.[19] SBA-15 showed much less adsorption capacity due to less ionic character of its surface, i.e. lower amount of deprotonated silanols, after the block copolymer templated synthesis of SBA-15 in acidic environment.

Deer et al. reported on cyano-modified mesoporous silica material with 13 nm wide-mesopores,[20,21] which was obtained by incorporating 2-cyanoethyltriethoxysilane during the synthesis of MCM-41 material. The obtained material was showcased as amenable for loading cytochrome c, which was demonstrated as the most efficient for this purpose when compared to the analogues with smaller mesopores.

Cage-like, cubic mesoporous silica materials, designated as FDU-12, were also constructed which contained large cavities (10-12.4 nm), with the size of entrances to the cavities adjustable in the range 4-9 nm.[22] The ability of the materials to adsorb lysozyme was shown to increase with the increase in the entrance size. 3D bicontinuous cubic Ia3d-type mesoporous silica (FDU-5 material with pores (4.5-9.5 nm)) was also synthesized in acidic medium at room temperature by using a nonionic triblock copolymer as template.[23]

MCM-48 is a silicate material containing cubic arrangement of mesopores, synthesized by ionic surfactant template method in basic environment. Kim et al. demonstrated that by including n-butanol as a co-solute and by changing the silicate/n-butanol ratio various silicate structures can

be obtained,[24] while increase in temperature of the reaction leads to widening of the pore diameter in the range 4.5 -10 nm. Pore swelling in the mesoporous materials had been achieved as well by addition of long chain alkanes,[25] while Rey et al. demonstrated a new mechanism for expansion of the mesopores, by addition of tetramethyl- and tetraethylammonium ions.[26]

A review article was recently published which demonstrates applicability of various pore-swelling agents, and the change in other synthesis parameters to obtain mesoporous silica materials with various pore sizes.[27] Implementation of various pore-swelling agents in SBA-15 and FDU-12-type materials is represented on Figure 1. In case of utilization of block copolymer surfactants with high fractions of the hydrophobic block (e.g. P123, $EO_{20}PO_{70}EO_{20}$), it is beneficial to use swelling agents with low or moderate solubility in the micelles, in order to avoid excessive swelling. However, application of surfactants with low fractions of the hydrophobic block (e.g., F127, $EO_{106}PO_{70}EO_{106}$) gives better large pore mesoporous silica structures with more soluble swelling agents.

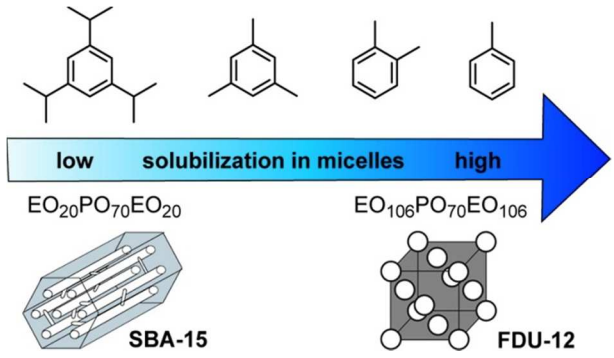

Fig. 1 Application of different pore-swelling agents in SBA-15 and FDU-12 type materials. Reprinted with permission from: M. Kruk, *Acc. Chem. Res*., 2012, **45**, 1678-1687. Copyright (2012) American Chemical Society.

Synthesis of large pore-mesoporous silica nanoparticles for adsorption and delivery of large drug molecules, proteins and enzymes

Nanoparticulate analogues of large-pore mesoporous silicates were sought-after in order to increase the efficiency of materials for applications in catalysis, separation and sequestration and delivery of macromolecules. This goal was first achieved by Han and Ying in 2005 through particle size-limitation with cationic fluorocarbon surfactant.[28] The authors synthesized a series of LPMSN materials with high surface area by application of different Pluronic block copolymers as templating agents, while TMB was applied as pore-swelling agent for construction of certain materials. By changing the synthesis conditions LPMSN materials with 3D cubic, 2D hexagonal, MCF-type and disordered packing of the mesopores were obtained with different pore sizes (5.2-19.5 nm). Synthesis of contemporary nanoparticulate mesoporous silicate materials is typically achieved by limiting the amount of silica precursors and by performing the synthesis for a short period (predominantly 2h) in high dilution, which limits the growth of the nanoparticles. Table 1 contains the list of different types of nanoparticulate materials covered in this review article along with their synthetic conditions, structural characteristics and demonstrated applications. Sun et al. synthesized LPMSN by tuning the TEOS/P123 molar ratio of the octane/water/P123/TEOS quadruple emulsion system,[29] which produced nanoparticles 50–80 nm wide and 100–200 nm long, with ordered large mesopores that are 13 nm in diameter. This material was shown capable to sequester enzymes from the environment much faster than the conventional SBA-15. Similar SBA-15-type nanorods with 80-200 nm in length and 10-26 nm wide were recently prepared by controlling acidic pH of the reaction mixture.[30] The material exhibited high affinity for adsorption of biomolecules and excellent uptake by the cells and biocompatibility in concentrations up to 200 μg/mL.

Table 1. Synthetic conditions, structural characteristics and demonstrated applications of different nanoparticulate LPMMSN materials (SA: surface area [m^2/g], PD: pore diameter [nm], PS:particle size [nm])

Type of material	Synthesis method	Characteristics	Comment	Application	Ref.
LPMSN	CTAB-templated, postsynthetic hydrothermal treatment with TOPO	SA: 407 PD: 8 PS:180	Rough surface, Irregular porosity	PET	10
LPMSN/polymer composite	CTAB-templated, *in situ* TMB addition	SA: 1040 PD: 4.7 PS:100 ±15	MCM-41 type	Growth factor loading, neural tissue regeration	11
LPMSN/collagen composite	CTAB/TOMAB co-templated	SA: 1265 PD (bimodal): 15.9; 2.3 PS:300	Irregularly structured porosity	Protein/NGF adsorption, neural tissue engineering	12
Series of LPMSNs	Pluronic-templated, *in situ* TMB addition, fluorocarbon surfactant mediated	SA:575-821, PD: 5.2-19.5 PS:50-400	Cubic, hexagonal, mesocellular foam	/	28
LPMSN	octane/water/P123/TEOS	SA:565 PD: 13 PS:50-200	Rod-shaped, regular porosity	Adsorption of lysozyme	29
Series of LPMSNs	P123/TMOS, acidic conditions	SA:707-867 PD: 7.0-8.3 PS:10-200	SBA-15 type rods	Protein adsorption, cellular uptake	30
LPMSN	CTAB-templated, *in situ* TMB addition	SA: 1061 PD (bimodal): 5.4; 14.5 PS:50 - 900	MCM-41 type, Wide distribution of PS	Cytochrome c delivery to cancer cells	31
HMM (LPMSN)	CTAB/TEOS/polymerization of styrene/aminoacid catlyst/octane	SA: ca. 600, PD: 4-20 PS:20-150	Tunable particle suze and pore diameter	Delivery of drug telmisartan	32 33
LPMSN	Postsynthetic etching of MCM-41 type MSN with aqueous $NaBH_4$	SA: N/A, PD: 3.0-9.7 PS:100-500	No record of SA, partial loss of porosity and structuration	Delivery of paclitaxel to cancer cells	34 35
Ultra-LPMSN	Postsynthetic etching of MCM-41 type MSN with methanolic solution of calcium nitrate or magnesium nitrate	SA: 312, 425 PD(bimodal): 4- 50 PS: ca. 200	Irregular pore structure	Adsorption of large proteins and antibodies	36
Series of LPMSNs	CTA^+ with tosilate or bromide counterions with small organic amines for templating	SA: 435-837 PD: 1.6- 5.4 PS: 40-130	Tunable large scale synthesis, different porsity	/	37
LPMSN	Dimethylphosphonatoethyl-trimethoxysilane/TEOS/ base/CTAB pore-templating	SA: 772 PD: 11,1 PS: 70-90	Raspberry pore morphology	Adsorption of bovine serum albumin	38
Series of LPMSN	Tannic acid-templating in ethanol/NH_4OH	SA: 420-560 PD: 6-13 PS: 200	Measured encapsulated enzyme activity	Adsorption of differently sized proteins	39
Series of LPMSN	DMHA/CTAB/OTAB pore templating, F127 for regulation of particle size	SA: ca. 1000 PD: 2.7-4.6 PS: ca. 200	Regular porosity Increased cyt c loading with pore diameter	Adsorption of cytochrome c and delivery to cancer cells	40
LPMSN	TOMAB/CTAB-pore templating	SA: ca. 1280 PD: 17.4	Irregular porosity	Adsorption of cytochrome c	42

		PS: ca. 280	Cyt c loading 50 wt%		
Series of LPMSN	pore-swelling alkanes/etanol/NH_4OH/H_2O/ CTAB	SA: ca. 1200 PD: 2.5 - 8.8 PS: 50-100	Enzyme activity improved upon confinement in mesopores	Adsorption of lysozyme, stability and activity	43 44
SBA-1 type LPMSN	hexadecyl pyridinium chloride-pore templating, complexed with poly(acrylic acid). TMB-pore expansion	SA: ca. 800 PD: 3.8 – 5.3 PS: 100-130	Cubic pore arrangement	Adsorption of lysozyme, activity against bacterial cell wall	45
LPMSN	pore-templating with Pluronic P104	SA: N/A PD: 6.5 PS: 300x500	Entrapped enzyme shows size selective activity	Porcine liver esterase loaded, gated nanodevice	46
LPMMSN	Magnetite nanoparticles/CTAB/TMB-pore expansion	SA: 959 PD: 12.4 PS: 80-750	Core/shell, radial porous structure	/	48
SBA-15 type LPMMSN	P123/NaCl/H_2O/EtOH/TEOS	SA: 46 PD: 7 PS: ca. 600	Very low SA and pore volume	Loading of large drug rapamycin	49
LPMMSN	CTAB templating, decane/TMB as pore expanders	SA: 700–1100 PD: 3.8–6.1 PS: 40–70	Core/shell, radial porous structure	loading of DNA, MRI, drug delivery	50 51
LPMMSN	Pluronic P123/CTAB-templating, acidic conditions	SA: 190 – 250 PD:4.3- 4.5 PS: ca. 300	High magnetization (29.3 emu/g)	removal of toxic microcystin-LR	52
SBA-15, FDU-12 type LPMSN, LPMMSN	macroporous carbon-PS templating, P123(or F127)/TEOS /(magnetite NP) in ethanol/water	SA: 790, 280 PD: 8, 7 PS: 450	Highly uniform spheres	Microcystin removal from water	53
LPMMSN	Hexadecyltrimethylammonium *p*-toluene-sulfonate-pore templating, triethanolamine	SA: 464-596 PD(bimodal): 3.4; 7.9-12.5 PS: 150	Uniform morphology, radial porosity	Drug delivery, cell uptake, hyperthermia, gene delivery	54 55 56
Series of LPMMSN	TEOS/Pluronic F127/TMB /HCl/H2O, fluorocarbon FC-4 for PS templating	SA: 201-716 PD: entr. 3.7-17.3, cav. 12.2-20.5 PS: 70-300	Smaller entrance size, bigger cavity, different porous structures	Plasmid DNA loading and stability against nucleases	57
Ultra-LPMSN	Postsynthetic treatment of MSN with TMB at 140˚C for 4 days in autoclave	SA: 395 PD: 23 PS: 200	Irregular porous structure	Loading siRNA. Knockdown of GFP and VEGF genes *in vivo*	58 59
LPMSN, LPMMSN	TEOS/Pluronic F127/TMB /HCl/H2O, fluorocarbon FC-4 for PS templating	SA: 421-700 PD: 10.6 PS: 200	Impregnation of iron salts, in situ Fe_3O_4	Simultaneous drug and gene delivery	60 61 62
Series of LPMSN, LPMMSN	Polystyrene-b-poly (acrylic acid)/CTAB-pore templating H_2O/THF/EtOH/TEOS/NH_3	SA: 233-507 PD: 2.8-16 PS: 30-650	Uniform, hexagonal, cubic, lamellar, hollow porosity	Gene delivery, inhibition of VEGF, MRI	63
LPMSN	TEOS/APTES/CTAB/TMB/ decane/NH_3/ethylene glycol/H_2O	SA: 959 PD: 5.9 PS: 70	Radial porosity	Glutathione responsive delivery of oligonucleotides	64

Lin et al. showcased in 2007 the applicability of large pore MSN for delivery of membrane-impermeable cytochrome c to cancer cell lines.[31] The authors synthesized hexagonally structured silica nanoparticulate material which contained 5.4 nm-wide mesopores by including TMB as a pore-swelling agent during CTAB-templated synthesis of MSN. The material was demonstrated to enter the cancer cells and to deliver its cargo enzyme. The authors also showed that adsorption of the enzyme on silica surface did not change its activity, since the cytochrome c released from MSN showed the same activity as the enzyme which was not subjected to adsorption and desorption.

Spherical silica nanoparticles (Hiroshima Mesoporous Material, HMM) with a tunable pore size ranging from 4 to 15 nm and a tunable particle size in nanometer range (20–80 nm) were developed by using an organic template method in a water/oil phase.[32] Preparation of the material included simultaneous hydrolytic condensation of TEOS and the polymerization of styrene into polystyrene (PS). The process uses an amino acid as the catalyst, octane as the hydrophobic-supporting reaction component, and CTAB as the surfactant. Final wide pore silica nanoparticles (Figure 2) were obtained after removal of PS and CTAB by calcination. Similarly synthesized nanoparticles with pore diameter ranging from 4 to 20 nm and a controllable particle diameter ranging from 20 to 150 nm were tested for the ability to load and deliver drug telmisartan.[33] Strong correlation was noted between increasing pore diameter and increased loading and the rate of drug release.

Reaction of MSN material with $NaBH_4$ was also showcased to yield silica nanoparticles with enlarged mesopores.[34] Before the reaction MSN showed BJH pore diameter of 3 nm, while after reaction for 1 and 2 hours in aqueous suspension of $NaBH_4$, the BJH data revealed enlargement of pores to 5.6 and 10 nm, respectively. However, after the etching, intensity of BJH peaks

noticeably decreased indicating smaller number of pores, while TEM images and XRD data showcased the loss in structuration of the materials, which indicate difficulties in controlling the $NaBH_4$-induced etching procedure. Nevertheless, the authors successfully demonstrated applicability of the synthesized materials for *in vitro* treatment of cancer cells and *in vivo* kinetics of drug release with paclitaxel-loaded materials.[35] Etching of the mesopore walls was also demonstrated by reaction with methanolic solution of calcium nitrate or magnesium nitrate.[36] The process led to widening of the mesopores, but also to formation of ultra-large pores with the average pore diametes of around 50 nm, which were the product of collapsing neighboring mesopores. Application of ultra-large pore MSN in adsorption of large proteins and antibodies was demonstrated.

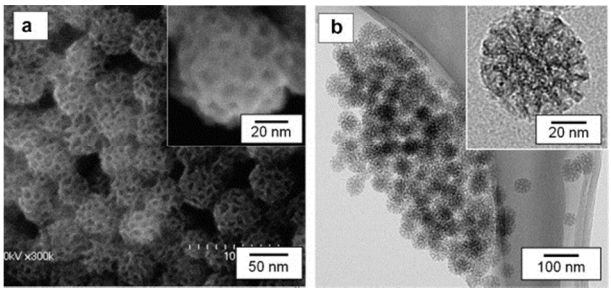

Fig. 2 SEM (a) and TEM (b) images of prepared LPMSNs. The inset image is a high-resolution electron microscope image of a single mesoporous silica nanoparticle. Reproduced with permission from ref. [32]

Large scale synthesis of MSNs was also recently reported, where the authors obtained nanoparticles with various arrangements of mesopores (stellate, raspberry, worm-like) with tunable pore-diameters.[37] The syntheses were performed by using cetyltrimethylammonium (CTA^+) as the templating surfactant, with tosilate or bromide counterions, and small organic amines (SOAs) as the mineralizing agent. Tosylate counterions favored stellate morphology

while bromide induced formation of raspberry structures at ultralow SOA concentrations. Both anions favored construction of nanoparticles with a wormlike morphology at high SOA concentrations. Raspberry morphology of large pore (11.1 nm in diameter) mesoporous silica nanoparticles were also synthesized by co-condensation of dimethylphosphonatoethyl-trimethoxysilane with TEOS in basic aqueous solution, with CTAB pore-templating.[38] The material exhibited high surface area (772 m^2/g) and particle sizes in the range 70-90 nm, which showed high affinity for adsorption of bovine serum albumin and formed very stable aqueous suspensions. The authors also obtained other various materials with different structures by changing the syntheses parameters.

Tannic acid (TA) was demonstrated as an excellent pore-templating agent, which facilitated construction of MSN with particle diameters around 200 nm and tunable size of mesopores (6-13 nm), accomplished by changing amount of TA in ethanol/NH_4OH reaction mixtures.[39] Application of TA is analogous to anionic surfactants since it contains multiple phenolic hydroxyl groups which are deprotonated in highly basic solutions and intermolecular π-π interaction between the aryl rings helps the self-assembly of individual TA molecules to template the mesopores. The prepared materials were also shown applicable for adsorption of differently sized proteins.

Pore-templating by a combination of N,N-dimethylhexadecylamine (DMHA) with CTAB or octadecyltrimethylammonium bromide (OTAB) (Figure 3) have been shown to produce MSNs with pore diameters of up to 4.6 nm.[40] In addition, the presence of block copolymer F127 was demonstrated to dictate the size of nanoparticles. Increasing the amount of F127 yielded in decreasing of particle diameters and in narrowing their size distribution. Sequestration of cytochrome c from a solution and its delivery to cancer cells was also successfully demonstrated.

The capability of various neutral alkylamines to expand the mesopores of silicate materials had been known since 1998.[41] The pore-expansion was noted by *in situ* formation of alkylamines through thermal degradation of mesopore-templating alkylammonium surfactant, by mixing the long chain-alkylamines with the surfactants or even by postsynthetic treatment of surfactant-containing mesoporous silicate materials.

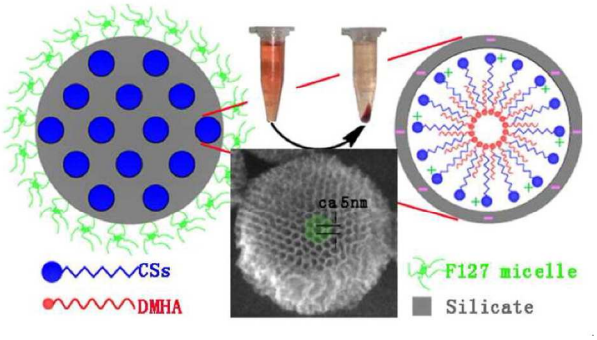

Fig. 3 Schematic representation of the MSN pore-templating by combination of DMHA and CSs (CTAB or OTAB). Sequestration of cytochrome c and TEM image of the synthesized MSN nanoparticles are also presented. Reproduced with permission from ref.[40]

Application of TOMAB as an auxiliary pore – templating surfactant, along with CTAB, was shown to produce nanoparticles with irregular porous structure, but pore diameter, pore volume and specific surface area of the material were very high, 17.4 nm, 5.9 cm^3/g and 1280 m^2/g respectively.[42] The material's maximum loading capacity for cytochrome c was determined as around 50 wt%. Alkanes, which were previously used as pore-swelling agents in mesoporous silicate materials,[25] have been demonstrated recently by Kao and Mou as applicable for construction of nanoparticulate mesoporous silica, which exhibit high affinity for loading lysozyme (42 wt%).[43] Ethanol was applied in this work to facilitate dispersion of long-chain alkanes inside the surfactant templates to induce the pore-swelling effect. A series of materials

with high surface area (ca. 1200 m^2/g) and regular and irregular porous structures with tunable pore diameters from 2.5 to 8.8 nm were obtained by studying application of different pore-swelling alkanes (hexane, octane, decane, dodecane and hexadecane) and by modifying amounts of ethanol and ammonia during the synthesis of the materials. The same research group subsequently reported that adsorption of lysozyme in the mesopores of LPMSN improves its stability toward heating-induced denaturation, while its activity toward hydrolysis of trisaccharide is much enhanced.[44] This improvement in the catalysis ability of the enzyme upon confinement inside the LPMSN mesopores was attributed to a small change in tertiary structure of the enzyme upon interaction with silica surface within the mesopores of suitable size, which improves the accessibility of the enzyme's active site. On the contrary, another research article reported that the ability of mesoporous silicate-adsorbed lysozyme to hydrolyze Micrococcus cell walls was inhibited if most of the enzyme was adsorbed inside the mesopores of LPMSN.[45] However, this result was a consequence of inability of the large cell wall to reach the lysozymes' active sites inside the mesopores. The authors synthesized SBA-1 nanomaterials with cubic arrangement of mesopores with hexadecyl pyridinium chloride (CPC) as pore-templating agent, complexed with anionic poly(acrylic acid) (PAA). Application of TMB during the synthesis yielded in expansion of the mesopores from the original 2.5 nm (without TMB) to the nanoparticulate materials with 3.8, 4.8 and 5.3 nm pore diameters, by increasing the amounts of TMB. Obtained particle sizes were in the range 100-130 nm and the highest specific surface area (798 m^2/g) was obtained for the material synthesized with the most amount of added TMB. Even though the material with the smallest pores (2.5 nm) adsorbed the least amount of the enzyme (165 mg/g), it showed the highest activity (24 % when compared to the free enzyme). For comparison, the material with bigger pore size (5.3 nm) exhibited higher enzyme loading (297 mg/g) but its activity was determined as 8.9 % of the activity of the free enzyme. Hence, in case

of small-pore material, the most of enzyme molecules were on the outside surface of nanoparticles and therefore available for the enzymatic activity against Micrococcus cell walls.

Attractive demonstration of size selective enzymatic activity of LPMSN-pore loaded porcine liver esterase (PLE) was recently reported by Xue and Zink.[46] The material with mesopore diameter of 6.5 nm was synthesized by pore-templating with Pluronic P104, and the pore entrances were functionalized with β-cyclodextrin through imine-containing linkers (Figure 4A). Star-like capping agent contained adamantane-moieties on each arm of the molecule, which have high affinity for forming inclusion complexes with surface functionalized β-cyclodextrins. After loading PLE and capping the mesopores, the activity of this enzyme was measured as a function of the substrate size. Smaller substrate-molecule was capable to diffuse into the capped mesopores (Figure 4B), which in fact exhibited amplification of the enzymatic activity since the ester-hydrolysis yielded acids which were capable of cleaving the imine linker. Hence, once the linker was cleaved more of the smaller-sized substrates and even the bigger substrate molecules were capable of entering the mesopores to yield the hydrolyzed products.

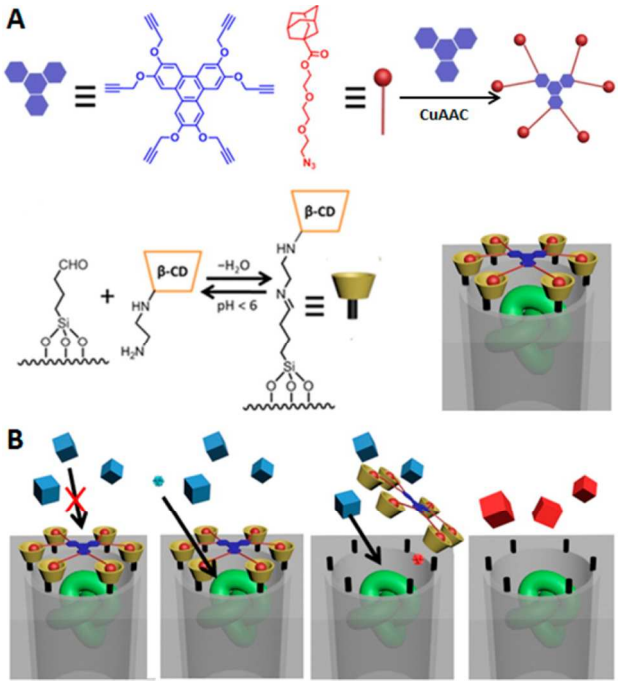

Fig. 4 Schematic representation of the construction of enzyme entrapped LPMSN-based nanosystem (A) and the mechanism of size selective self-amplifying activity (B). Reprinted with permission from: M. Xue and J. I. Zink, *J. Am. Chem. Soc.*, 2013, **135**, 17659-17662.. Copyright (2013) American Chemical Society.

Magnetic analogues of LPMSNs

Synthesis and application of magnetic MSN materials (MMSN) has been reviewed in detail recently.[47] Incorporation of magnetic nanoparticles as the core inside nanosized mesoporous silica shell is typically performed by including magnetic nanoparticles in the reaction mixture before addition of silica precursors. Extensive sonication of the suspension and pre-coating the surface of magnetic nanoparticles with small amount of TEOS or organosilane before formation of mesoporous silica shell usually ensures high dispersion and uniform distribution of magnetic nanoparticles in the core/shell materials. Addition of pore-swelling TMB during the synthesis of MMSN was also demonstrated as a viable route to obtain large pore analogs of these materials.[48]

The nanoparticulate material contained magnetic iron-oxide (maghemite) core and mesoporous silica shell with radial porous structure, high surface area (959 m^2/g), large average pore diameter (12.4 nm) and large pore volume (2.3 cm^3/g). Previously, Rosenholm et al. constructed LPMMSN materials of SBA-15 type, with pore sizes of 7 nm.[49] Even though the pore volume (0.08 cm^3/g) and specific surface area (46 m^2/g) of this material were very low, the authors demonstrated its applicability for loading a large drug Rapamycin inside the mesopores. The same research group also synthesized a series of LPMMSNs with CTAB templating, while TMB and decane were applied as pore-swelling agents in different ratios.[50] The nanoparticulate materials exhibited high surface area (up to 1100 m^2/g), radial porous structure and high capacity for loading salmon sperm DNA (375 mg/g). The nanoparticles were functionalized with polyethylene glycol (PEG) moiety, labeled with fluorescein, and the authors demonstrated that pore diameter has a strong influence on capacity of the material to serve for MRI and fluorescence imaging or drug delivery.[51]

Zhao et al. recently published the synthesis of large pore MMSN (LPMMSN) by templating the porous structure with triblock-copolymer Pluronic P123, with the assistance of a trace amount of CTAB.[52] The obtained material exhibited uniform pore diameters (4.5 nm), specific surface area in the range: 190 – 250 m^2/g, pore volumes in the range 0.17 – 0.38 cm^3/g and high magnetization (29.3 emu/g). This material was successfully implemented for removal of toxic microcystin-LR (2 nm in diameter) from water solution. The same research group developed synthesis of LPMSN and LPMMSN with narrow particle size distribution through templating method with three-dimensionally ordered macroporous carbon (3DOMC),[53] which was casted by carbonization of resol (ethanol solution of phenolic resin) on annealed sedimentation of uniform silica spheres, followed by etching of silica in basic solution. In case of application of core/shell

Fe_3O_4@SiO_2 nanoparticles, magnetic iron-oxide nanoparticles stayed on 3DOMC template after silica etching, which ultimately yielded Fe_3O_4@SBA-15 nanospheres (Figure 5). The monodispersed, large pore SBA-15 and Fe_3O_4@SBA-15 nanoparticles were formed by impregnation of 3DOMC or Fe_3O_4@3DOMC templates with a weakly acidic solution of Pluronic P123 and TEOS in ethanol/water mixture and by slow evaporation of ethanol during 24 h at 30 ˚C. The nanoparticles were then stabilized by hydrothermal treatment at 100 ˚C for 10 h in strong acidic environment, and liberated from the 3DOMC template and Pluronic P123 by calcination. As-synthesized SBA-15 and Fe_3O_4@SBA-15 nanoparticles were 450 nm in diameter and exhibited surface area of 790 m^2/g and 280 m^2/g, pore volumes of 0.98 cm^3/g and 0.404 cm^3/g, and pore diameters of 8 nm and 7 nm, respectively.

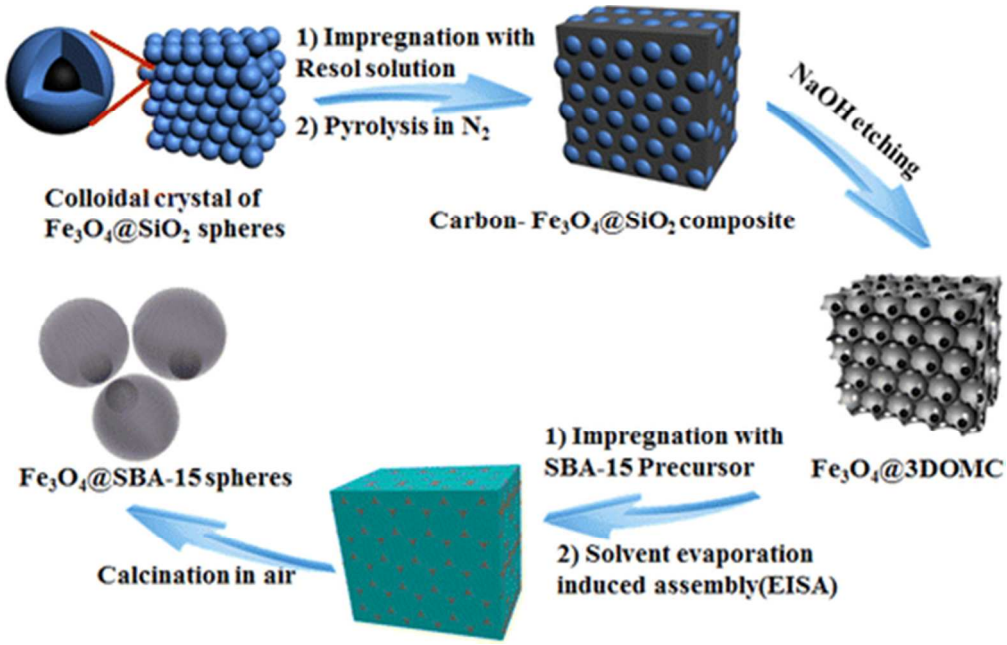

Fig. 5 Synthesis pathway of Fe_3O_4@SBA-15 nanoparticles by templating with Fe_3O_4@3DOMC. Reprinted with permission from: M. Wang, Z. Sun, Q. Yue, J. Yang, X. Wang, Y. Deng, C. Yu and D. Zhao, *J. Am. Chem. Soc.*, 2014, **136**, 1884-1892. Copyright (2014) American Chemical Society.

Hexadecyltrimethylammonium *p*-toluene-sulfonate (CTAT) was recently used as a templating surfactant for the synthesis of core/shell LPMMSN material, which was characterized by bimodal distribution of mesopores (smaller 3.2-3.4 nm and bigger 7.9-12.5 nm pores), oriented in radial manner.[54] The authors have proven the capability of the material to release surface-adsorbed doxorubicin upon acidification of the environment while application of alternating magnetic field was capable to elevate the temperature of the surrounding medium. Hence, the constructed materials may find application in combination chemo/hyperthermia. Similar CTAT-templated synthesis produced monodispersed LPMMSN nanoparticles of 150 nm in diameter with radial orientation of the mesopores.[55] The material also exhibited bimodal distribution of mesopore sizes (3.4 and 10.7 nm), high surface area (462.4 m^2/g) and saturation magnetization of 6.5 emu/g. After grafting amine moiety on the surface of the nanoparticles, zeta potential of the surface changed to positive value which allowed loading of **C**ytosine triphosphate deoxynucleotide-Guanine tri**p**hosphate deoxynucleotide (CPG) oligonucleotide (CPG ODN). This oligonucleotide is known to promote production of immunostimulant cytokines. Indeed, CPG/NH_2-LPMMSN was demonstrated to induce production of inteleukin-6 (IL-6) in cells, which can be applied for promotion of immune response on unhealthy cells. The same research group also reported the use of similarly synthesized LPMSN nanomaterials for successful delivery of immunostimulatory double-stranded DNA (dsDNA) to the cells in order to trigger cytosolic DNA sensors for activation of type I interferons (IFN).[56]

Gene delivery by large pore mesoporous silica nanomaterials

The first study on applicability of amine-functionalized-LPMSN materials, with pore diameters of up to 20.5 nm, for loading plasmid DNA (pDNA) and demonstration of their capability to preserve the pDNA molecules in the presence of nucleases was reported in 2009.[57] The result indicated that nucleic acids can be effectively protected from the nucleases from the bloodstream by loading them inside the large pores of LPMSN, which is one of the important aspects in construction of gene delivery vehicles. Usefulness of LPMSN materials for *in vitro* and *in vivo* gene delivery is undoubtedly demonstrated by Min et al.[58] Small interfering RNA (siRNA) molecules were adsorbed on amine-functionalized MSN materials containing small (2.1 nm) and large (23 nm) mesopores and after exposure to RNase for 2 h only siRNA which was adsorbed inside the mesopores of LPMSN could still be detected as intact. The siRNA-loaded LPMSN material, which was also functionalized with an imaging dye and a PEG moiety, was further demonstrated to efficiently (more efficiently then commercially available lipofectamine 2000) lead to gene silencing by inhibiting expression of green fluorescent protein (GFP) in HeLa cells. Downregulation of a therapeutically relevant vascular endothelial growth factor (VEGF) was also demonstrated *in vitro* and *in vivo*, which is a signaling protein for activation of angiogenesis and hence of critical importance for the proliferation of tumor tissues. Figure 6 shows the schematic representation of siRNA delivery to cells and the influence of VEGF gene silencing by siVEGF-P-T-MSN23 (siVEGF stands for siRNA silencing the expression of VEGF gene, P = PEG moiety, T = imaging dye TAMRA, MSN23 = MSN material with 23 nm pore diameter) on tumor volume when compared to injection of naked siVEGF and PBS. The same research group previously showcased the ability of LPMSN to protect plasmid DNA (pDNA) from nuclease

activity and efficient *in vitro* transfection efficacy of pDNA-encoding green fluorescent protein (GFP) and luciferase.[59]

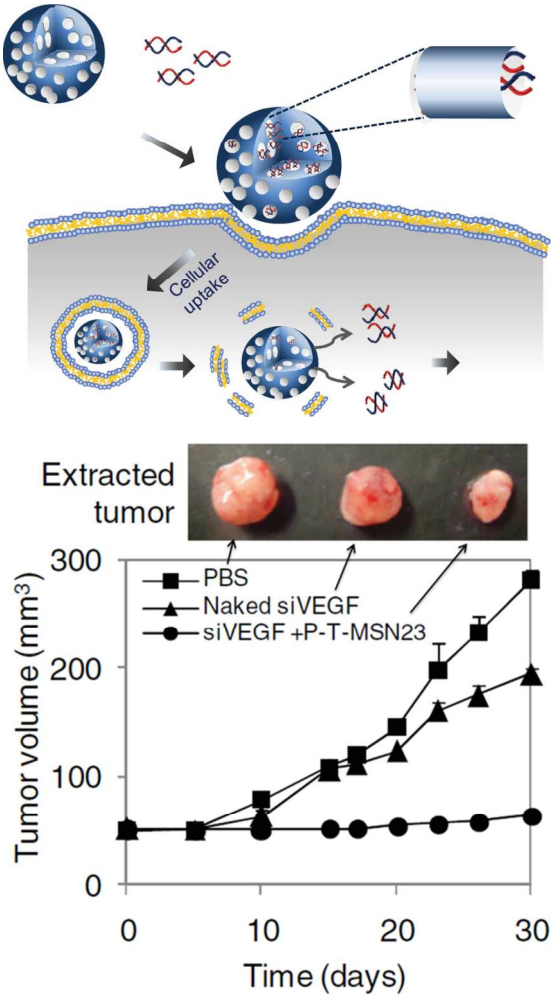

Fig. 6 representation of siRNA delivery to cells and the graph showing the tumor volume as a consequence of VEGF gene silencing by siVEGF-P-T-MSN23, in comparison to addition of PBS solution of siVEGF and only PBS solution. Extracted tumors at day 30 are shown for size comparison. Reproduced with permission from the reference.[58]

Hartono et al. synthesized cubic LPMSN material with pore size of 11 nm by the method of Han and Ying,[28] functionalized it with degradable cationic polymer poly(2-dimethylaminoethyl acrylate (PDMAEA) and applied it for simultaneous drug and gene delivery.[60] The functionalized polymer slowly hydrolyzes in physiological conditions to release the charged moiety 2-

dimethylammoniumethanol, which consequently yields in release of nucleic acids and the mesopore loaded drugs from the LPMSN material. The same research group demonstrated application of poly-L-lysine (PLL) functionalized LPMSN material for the delivery of therapeutic siRNA to inhibit the proliferation of osteosarcoma cancer cells.[61] Furthermore, the research group developed magnetic gene delivery system by functionalization of LPMMSN with polyethyleneimine (PEI).[62] Gene silencing was once more successfully demonstrated on osteosarcoma cancer cells, which led to inhibition of their viability. Application of magnetic field was also demonstrated to enhance the uptake of the magnetic material by the cells.

The research group of Jianlin Shi demonstrated recently application of LPMSN material for delivery of plasmid DNA.[63] The authors firstly synthesized various LPMSN materials with different mesostructures (hexagonal, cubic, lamellar) by modification of the ratio of pore-templating polystyrene-b-poly(acrylic acid) and CTAB, which also yielded in a flower-like morphology of the nanoparticles (Figure 7). Loading of magnetite nanoparticles inside the large mesopores of the material was further showcased and magnetic resonance imaging with the as-constructed composite was achieved. After surface functionalization with amine moieties, LPMSN material was loaded with pDNA and its capability for *in vitro* and *in vivo* transfection was demonstrated. Expression of pDNA-encoding green fluorescent protein (GFP) was achieved *in vitro* in cancer cells, while plasmid DNA was also applied for *in vivo* delivery of RNA-interference and inhibition of VEGF.

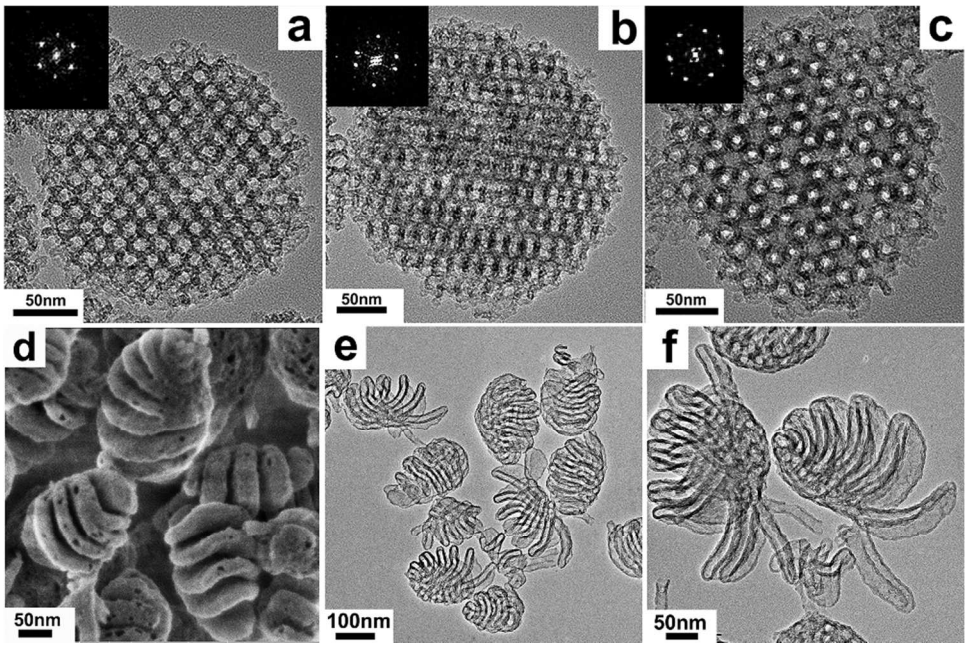

Fig. 7 TEM images and corresponding Fourier diffractograms (insets) of hexagonal LPMSN along the [110] (a) [311] (b) and [111] (c) directions. (d) SEM and (e, f) TEM images of flower-like LPMSN. Reproduced with permission from ref.[61]

Stimulus responsive delivery of DNA oligonucleotides was reported recently by Rosenholm et al.[64] The authors prepared LPMSN with different pore sizes (3.5-5.7 nm) which contained amine functionality attached to the materials through a disulfide linker. After loading the oligonucleotides their release from the materials was demonstrated upon cleaving the disulfide bond with addition of glutathione.

Conclusions and Perspectives

Large pore MSN materials can be synthesized though different approaches, mainly by addition of agents which can cause the swelling of hydrophobic core or the spacing of hydrophilic heads of the surfacrant-constructed micelles, or by application of surfactants with longer hydrophobic

chains. Different morphologies of the nanomaterials may be obtained, with hexagonal, cubic, radial, lamellar or disordered packing of the mesopores. Large pore materials with large specific surface areas can be synthesized, which is important in light of possibilities for surface functionalization and the loading of the mesopores with large biomolecules. Applicability of LPMSN materials and their magnetic analogues (LPMMSN) for successful delivery of large molecules is clearly evident based on numerous examples of loading and delivery of enzymes, antibodies and nucleic acids, which do not change their activities after the processes of adsorption and desorption from the materials. A number of studies also demonstrate protective character of LPMSN materials, especially in preserving nucleic acids from the action of nucleases from the bloodstream.

Due to high surface areas, possibilities of construction of LPMSN materials with different morphologies, proven biocompatibility and due to ease of their functionalization and capability of loading with various molecules, these materials offer a plethora of possibilities for construction of functional nanoassemblies for various biomedical applications.

Acknowledgments

Nikola Knežević is thankful to Pôle Chimie Balard Fondation, Chaire Total, visiting scholar program, for financial support.

References

1 H. Yang, Q. Lu, F. Gao, Q. Shi, Y. Yan, F. Zhang, S. Xie, B. Tu and D. Zhao, *Adv. Funct. Mater.*, 2005, **15**, 1377-1384.

2 J. S. Beck, J. C. Vartuli, W. J. Roth, M. E. Leonowicz, C. T. Kresge, K. D. Schmitt, C. T. W. Chu, D. H. Olson and E. W. Sheppard, *J. Am. Chem. Soc.*, 1992, **114**, 10834-10843.

3 C.-Y. Lai, B. G. Trewyn, D. M. Jeftinija, K. Jeftinija, S. Xu, S. Jeftinija and V. S. Y. Lin, *J. Am. Chem. Soc.*, 2003, **125**, 4451-4459.

4 B. Tan and S. E. Rankin, *Langmuir*, 2005, **21**, 8180-8187.

5 T. Suteewong, H. Sai, R. Cohen, S. Wang, M. Bradbury, B. Baird, S. M. Gruner and U. Wiesner, *J. Am. Chem. Soc.*, 2010, **133**, 172-175.
6 N. Ž. Knežević, I. I. Slowing and V. S. Y. Lin, *ChemPlusChem*, 2012, **77**, 48-55.
7 P. Horcajada, A. Rámila, J. Pérez-Pariente and M. Vallet-Regi, *Microporous Mesoporous Mater.*, 2004, **68**, 105-109.
8 J. Lu, M. Liong, Z. Li, J. I. Zink and F. Tamanoi, *Small*, 2010, **6**, 1794-1805.
9 Q. He, Z. Zhang, F. Gao, Y. Li and J. Shi, *Small*, 2011, **7**, 271-280.
10 L. Miller, G. Winter, B. Baur, B. Witulla, C. Solbach, S. Reske and M. Linden, *Nanoscale*, 2014, **6**, 4928-4935.
11 Y. Cho, R. Shi, A. Ivanisevic and R. Ben Borgens, *Nanotechnology*, 2009, **20**, 275102.
12 J. H. Lee, J.-H. Park, M. Eltohamy, R. Perez, E.-J. Lee and H.-W. Kim, *RSC Adv.*, 2013, **3**, 24202-24214.
13 C. T. Kresge, M. E. Leonowicz, W. J. Roth, J. C. Vartuli and J. S. Beck, *Nature*, 1992, **359**, 710-712.
14 D. Zhao, J. Feng, Q. Huo, N. Melosh, G. H. Fredrickson, B. F. Chmelka and G. D. Stucky, *Science*, 1998, **279**, 548-552.
15 D. Zhao, Q. Huo, J. Feng, B. F. Chmelka and G. D. Stucky, *J. Am. Chem. Soc.*, 1998, **120**, 6024-6036.
16 P. Schmidt-Winkel, W. W. Lukens, D. Zhao, P. Yang, B. F. Chmelka and G. D. Stucky, *J. Am. Chem. Soc.*, 1998, **121**, 254-255.
17 Y.-J. Han, G. D. Stucky and A. Butler, *J. Am. Chem. Soc.*, 1999, **121**, 9897-9898.
18 J. Zhao, F. Gao, Y. Fu, W. Jin, P. Yang and D. Zhao, *Chem. Commun.*, 2002, 752-753.
19 H. Takahashi, B. Li, T. Sasaki, C. Miyazaki, T. Kajino and S. Inagaki, *Microporous Mesoporous Mater.*, 2001, **44–45**, 755-762.
20 J. Deere, E. Magner, J. G. Wall and B. K. Hodnett, *Chem. Commun.*, 2001, 465-465.
21 J. Deere, E. Magner, J. G. Wall and B. K. Hodnett, *J. Phys. Chem. B*, 2002, **106**, 7340-7347.
22 J. Fan, C. Yu, F. Gao, J. Lei, B. Tian, L. Wang, Q. Luo, B. Tu, W. Zhou and D. Zhao, *Angew. Chem. Int. Ed.*, 2003, **42**, 3146-3150.
23 X. Liu, B. Tian, C. Yu, F. Gao, S. Xie, B. Tu, R. Che, L.-M. Peng and D. Zhao, *Angew. Chem. Int. Ed.*, 2002, **41**, 3876-3878.
24 T.-W. Kim, F. Kleitz, B. Paul and R. Ryoo, *J. Am. Chem. Soc.*, 2005, **127**, 7601-7610.
25 J. L. Blin, C. Otjacques, G. Herrier and B.-L. Su, *Langmuir*, 2000, **16**, 4229-4236.
26 A. Corma, Q. Kan, M. T. Navarro, J. Pérez-Pariente and F. Rey, *Chem. Mater.*, 1997, **9**, 2123-2126.
27 M. Kruk, *Acc. Chem. Res.*, 2012, **45**, 1678-1687.
28 Y. Han and J. Y. Ying, *Angew. Chem. Int. Ed.*, 2005, **44**, 288-292.
29 J. Sun, H. Zhang, R. Tian, D. Ma, X. Bao, D. S. Su and H. Zou, *Chem. Commun.*, 2006, 1322-1324.
30 Y. Yang, S. Karmakar, J. Zhang, M. Yu, N. Mitter and C. Yu, *J. Mater. Chem. B*, 2014, **2**, 4929-4934.
31 I. I. Slowing, B. G. Trewyn and V. S. Y. Lin, *J. Am. Chem. Soc.*, 2007, **129**, 8845-8849.
32 A. B. D. Nandiyanto, S.-G. Kim, F. Iskandar and K. Okuyama, *Microporous Mesoporous Mater.*, 2009, **120**, 447-453.
33 Y. Zhang, Z. Zhi, T. Jiang, J. Zhang, Z. Wang and S. Wang, *J. Controlled Release*, 2010, **145**, 257-263.
34 L. Jia, J. Shen, Z. Li, D. Zhang, Q. Zhang, C. Duan, G. Liu, D. Zheng, Y. Liu and X. Tian, *Int. J. Pharm.*, 2012, **439**, 81-91.
35 L. Jia, J. Shen, Z. Li, D. Zhang, Q. Zhang, G. Liu, D. Zheng and X. Tian, *Int. J. Pharm.*, 2013, **445**, 12-19.
36 H.-S. Shin, Y.-K. Hwang and S. Huh, *ACS Appl. Mater. Interfaces*, 2014, **6**, 1740-1746.

37 K. Zhang, L.-L. Xu, J.-G. Jiang, N. Calin, K.-F. Lam, S.-J. Zhang, H.-H. Wu, G.-D. Wu, B. Albela, L. Bonneviot and P. Wu, *J. Am. Chem. Soc.*, 2013, **135**, 2427-2430.
38 S. P. Maddala, D. Velluto, Z. Luklinska and A. C. Sullivan, *J. Mater. Chem. B*, 2014, **2**, 903-914.
39 Z. Gao and I. Zharov, *Chem. Mater.*, 2014, **26**, 2030-2037.
40 J. Gu, K. Huang, X. Zhu, Y. Li, J. Wei, W. Zhao, C. Liu and J. Shi, *J. Colloid Interface Sci.*, 2013, **407**, 236-242.
41 A. Sayari, M. Kruk, M. Jaroniec and I. L. Moudrakovski, *Adv. Mater.*, 1998, **10**, 1376-1379.
42 M. Eltohamy, U. S. Shin and H.-W. Kim, *Mater. Lett.*, 2011, **65**, 3570-3573.
43 K.-C. Kao and C.-Y. Mou, *Microporous Mesoporous Mater.*, 2013, **169**, 7-15.
44 K.-C. Kao, T.-S. Lin and C.-Y. Mou, *J. Phys. Chem. C*, 2014, **118**, 6734-6743.
45 J. Xu, W. Liu, Y. Yu, J. Du, N. Li and L. Xu, *RSC Adv.*, 2014, **4**, 37470-37478.
46 M. Xue and J. I. Zink, *J. Am. Chem. Soc.*, 2013, **135**, 17659-17662.
47 N. Z. Knezevic, E. Ruiz-Hernandez, W. E. Hennink and M. Vallet-Regi, *RSC Adv.*, 2013, **3**, 9584-9593.
48 N. Ž. Knežević, *Process. Appl. Ceram.*, 2014, **8**, 109-112.
49 J. M. Rosenholm, J. Zhang, W. Sun and H. Gu, *Microporous Mesoporous Mater.*, 2011, **145**, 14-20.
50 J. Zhang, X. Li, J. M. Rosenholm and H.-C. Gu, *J. Colloid Interface Sci.*, 2011, **361**, 16-24.
51 J. Zhang, J. M. Rosenholm and H. Gu, *ChemPhysChem*, 2012, **13**, 2016-2019.
52 Z. Sun, Q. Yue, Y. Liu, J. Wei, B. Li, S. Kaliaguine, Y. Deng, Z. Wu and D. Zhao, *J. Mater. Chem. A*, 2014, **2**, 18322-18328.
53 M. Wang, Z. Sun, Q. Yue, J. Yang, X. Wang, Y. Deng, C. Yu and D. Zhao, *J. Am. Chem. Soc.*, 2014, **136**, 1884-1892.
54 C. Tao and Y. Zhu, *Dalton Trans*, 2014, **43**, 15482-15490.
55 C. Tao, Y. Zhu, X. Li and N. Hanagata, *RSC Adv.*, 2014, **4**, 45823-45830.
56 C. Tao, Y. Zhu, Y. Xu, M. Zhu, H. Morita and N. Hanagata, *Dalton Trans*, 2014, **43**, 5142-5150.
57 F. Gao, P. Botella, A. Corma, J. Blesa and L. Dong, *J. Phys. Chem. B*, 2009, **113**, 1796-1804.
58 H. K. Na, M. H. Kim, K. Park, S. R. Ryoo, K. E. Lee, H. Jeon, R. Ryoo, C. Hyeon and D. H. Min, *Small*, 2012, **8**, 1752-1761.
59 M.-H. Kim, H.-K. Na, Y.-K. Kim, S.-R. Ryoo, H. S. Cho, K. E. Lee, H. Jeon, R. Ryoo and D.-H. Min, *ACS Nano*, 2011, **5**, 3568-3576.
60 S. B. Hartono, N. T. Phuoc, M. Yu, Z. Jia, M. J. Monteiro, S. Qiao and C. Yu, *J. Mater. Chem. B*, 2014, **2**, 718-726.
61 S. B. Hartono, W. Gu, F. Kleitz, J. Liu, L. He, A. P. J. Middelberg, C. Yu, G. Q. Lu and S. Z. Qiao, *ACS Nano*, 2012, **6**, 2104-2117.
62 B. H. Sandy, Y. Meihua, G. Wenyi, Y. Jie, S. Ekaterina, W. Xiaolin, Q. Shizhang and Y. Chengzhong, *Nanotechnology*, 2014, **25**, 055701.
63 D. Niu, Z. Liu, Y. Li, X. Luo, J. Zhang, J. Gong and J. Shi, *Adv. Mater.*, 2014, **26**, 4947-4953.
64 J. Zhang, M. Niemela, J. Westermarck and J. M. Rosenholm, *Dalton Trans.*, 2014, **43**, 4115-4126.